Removal of thiols from model jet-fuel streams assisted by ionic liquid membrane extraction

Ana R. Ferreira [a,b], Luísa A. Neves [a], Jorge C. Ribeiro [c], Fernando M. Lopes [c],
João A.P. Coutinho [b], Isabel M. Coelhoso [a], João G. Crespo [a,*]

[a] CQFB/REQUIMTE, Departamento de Química, FCT, Universidade Nova de Lisboa, 2829-516 Caparica, Portugal
[b] CICECO, Departamento de Química, Universidade de Aveiro, 3810-193 Aveiro, Portugal
[c] Galp Energia, Refinaria de Matosinhos, 4452-852 Leça da Palmeira, Matosinhos, Portugal

HIGHLIGHTS

- Ionic liquids are proved as alternative solvents for jet-fuel desulfurization.
- Target thiol is selectively extracted from n-dodecane (jet-fuel model compound).
- Ionic liquid and n-dodecane exhibit low mutual solubility preventing losses of fuel.
- Successful membrane-assisted extraction of target thiol from jet-fuel model system.

GRAPHICAL ABSTRACT
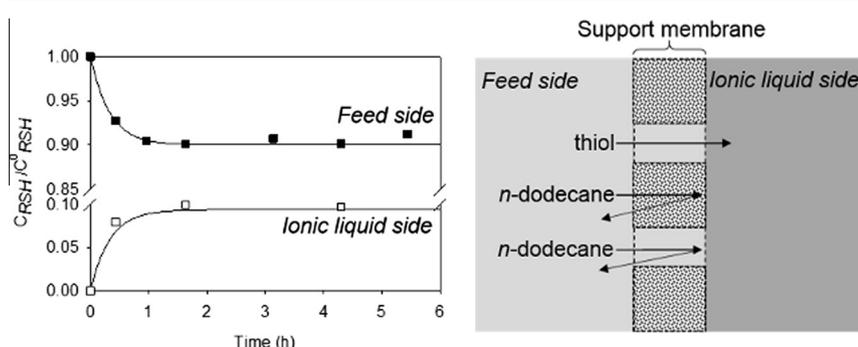
ARTICLE INFO

ABSTRACT

This work focuses on the use of ionic liquids as alternative solvents for the removal of thiols, at room-temperature, from n-dodecane used as jet fuel model stream. The model extraction system composed by a selected ionic liquid, the thiol to be removed and an alkane representative of the jet-fuel, show high selectivities and low distribution ratios, which makes unfeasible the use of conventional liquid–liquid extraction processes due to the high volume of ionic liquid required. This works evaluates the use of supported ionic liquid membranes (SILMs) for the selective removal of thiols applying vacuum in the downstream side. This approach consists in the incorporation of the ionic liquid inside the membrane pores, while due to the vacuum applied, the thiol compound is scrubbed. To study the target solute transport from the feed to the ionic liquid, extraction experiments were carried out using different 1-ethyl-3-methylimidazlium cation-based ionic liquids. The mass transfer resistance was found to be higher in the ionic liquid phase, which results mainly from the high ionic liquid viscosities, hindering the thiol transport.

The SILMs stability was investigated by evaluating different membrane supports, with the various ionic liquids selected for study. The results obtained show that the ionic liquids were properly incorporated inside the pores of the membrane support. However, and despite the negligible mutual solubility between n-dodecane and the studied ionic liquids, n-dodecane permeation through the membrane support was found to be undesirably high. This problem was solved by using a membrane contactor with polypropylene hollow fibre membranes, not wetted by the ionic liquid, which receives the thiol compound transported. Under these conditions, n-dodecane was not detected in the receiving ionic liquid phase.

© 2014 Elsevier B.V. All rights reserved.

* Corresponding author. Tel.: +351 212 948 300; fax: +351 212 948 550.
E-mail address: jgc@fct.unl.pt (J.G. Crespo).

1. Introduction

Petroleum industries are committed on reducing their sulfur emissions and improve or develop new desulfurization technologies, both to comply with regulatory requirements, and to optimize the fuel economy and conquer a superior treatment capacity.

Sulfur species, produced from fuel burning, are major pollutants responsible for severe environmental and health problems, which directed legislation towards more stringent limits on the fuel sulfur content, envisaging the use of ultra-low sulfur fuels. Further, the presence of these sulfurous compounds on fuel acts as a catalyst poison either on the fuel engine's exhaust emissions control systems, as in catalyst-aided refinery processes [1]. However, the availability of crude reserves with superior quality, i.e., with low sulfur content, diminished making refining industries prospect crudes with heavier and sourer compositions. The sulfur levels on these crudes can reach values almost up to 3.5% wt., that are much higher than those found on the light and sweet crudes, commonly treated due to their relative easy and cheap desulfurization [2]. Obviously, this quality deterioration on the supply side, and the more strict fuel specifications on the demand side, hinder the capacity and efficiency of conventional desulfurization processes (hydrocracking or hydrotreating processes), demanding an upgrade of the current processes [3].

The challenges presented are being pursuit by several research groups, and comprise the development of more active catalysts for the traditional catalytic hydrodesulfurization, and new alternatives such as oxidative, adsorptive, extractive and biological desulfurization processes, and their combinations [2,4–13]. Among these, liquid–liquid extraction appears to be an attractive alternative related with the moderate operating conditions (low temperature and pressure) and low energy cost. Regarding the extracting solvents, ionic liquids have shown a great potential on substituting the conventional volatile organic solvents used [4,14–23] due to their negligible volatility, liquid state at a wide temperature, including room temperature, high thermal and chemical stabilities, among others [24]. Moreover, being composed by bulky and asymmetric organic cations and organic or inorganic anions, their endless possible combinations rise as another key characteristic, the ability of tailoring their physical, chemical and solvation properties, towards a specific application.

Taking the latest into account, our previous work [25] presented an intensive ionic liquid screening aiming to understand and select the most suitable ionic liquid as extracting solvent for the removal of thiols from kerosene, by experimental and COSMO-RS predictions of liquid–liquid equilibrium, selectivity and distribution ratio. Based in the ternary system model considered of ionic liquid, 1-hexanethiol and n-dodecane, it was found that these systems present a very high selectivity towards the target thiol compound, due to the almost negligible mutual solubility of the ionic liquid and the n-alkane studied. This is a remarkable feature since mutual contamination and losses of fuel and ionic liquid can be avoided in the separation process. Nevertheless, the thiol distribution ratios observed towards the ionic liquids tested were lower than unit, imposing extremely large volumes of ionic liquid in the liquid–liquid extraction process in order to attain the desired separation.

Yet, it is important to reiterate that, in spite of the unfavorable aspect referred, the difference between the thiol and alkane solubilities in the ionic liquid still qualifies the use of ionic liquids as a solvent in separation processes regulated by mass transfer kinetics, or by combining it with an efficient regeneration process.

For this purpose, membrane assisted extraction using supported ionic liquid membranes (SILMs) is considered a potential separation process, as suggested by several works that used an immobilized ionic liquid phase either for gas separation, [26–28] or liquid–liquid

extraction [29–32]. SILMs result from the immobilization of a selected ionic liquid, which acts as the selective medium, on a polymeric or ceramic porous support, responsible for the mechanical resistance of the membrane. By using an ionic liquid supported in a porous membrane, it is possible to provide a short diffusion path for the transport of the target thiol solute from the jet-fuel feed phase to a receiving compartment. Other advantages are the solvent volume required, much lower than in a conventional liquid–liquid extraction and, additionally, the low mass transfer resistance when compared with solid membranes [26,31,33–37].

In this work, making use of the non-volatility of ionic liquids, the thiol transport is driven by a chemical potential gradient across the SILM, by reducing the target solute concentration in the receiving compartment, where a reduced vacuum pressure is applied. The thiol permeates selectively across the liquid membrane from the liquid feed phase to the vapor phase in the permeate side. This approach assures a simultaneous extraction and stripping in one single stage, avoiding the equilibrium restrictions previously identified in these systems.

The stability and lifetime performance of the SILMs have an important impact on their industrial potential use [36]. Due to their negligible volatility and very low affinity for the feed phase mixture, the use of ionic liquids reduces drastically the deterioration of SILMs in comparison with conventional supported liquid membranes where the evaporation or dissolution of solvent into the contiguous phases may occur. Still, the integrity of the SILMs prepared should be tested under pressure differences identical to the ones employed during the extraction/stripping process, in order to assure that the ionic liquid is not displaced from the porous support.

Taking into account all previous considerations, the work here developed started with the study of the diffusion and mass transfer of the target thiol compound from the n-dodecane jet-fuel model feed to the ionic liquid phase, by performing liquid–liquid extraction experiments. As referred before, thiol species show low solubility in the ionic liquids, limiting the extraction capacity of the ionic liquid, which turns more relevant the selection of the most promising ionic liquids based on their transport characteristics. Nonetheless, the concern with a possible co-extraction of valuable fuel constituents requires the use of ionic liquids based on imidazolium cations, with small alkyl side chains, to guarantee the lowest mutual solubility with the aliphatic hydrocarbon [25].

Since the application of SILMs depends from the membrane stability and selectivity behaviors, the previous ionic liquids were also tested with different support materials in order to find the SILM that fulfills the necessary requisites.

2. Mass transfer model

The liquid–liquid extraction experiments were performed using an adapted Lewis cell which allows the two phases contacting with a well-defined interface. These experiments consist in registering the solute concentration along time, which provides information about the 1-hexanethiol transport from the feed phase (rich in n-dodecane) to the ionic liquid phase.

During these experiments, it was assumed that at the interface, an equilibrium state is established. Therefore, a mass balance over the feed phase leads to the mass transfer of the 1-hexanethiol compound between the n-dodecane feed phase and the ionic liquid phase, described by the Eq. (1):

$$-V_f \frac{d(C_f)}{dt} = K_f A_i (C_f - C_f^*) \tag{1}$$

In this equation, V_f (m^3) is the feed phase volume, C_f and the C_f^* (mol m^{-3}) are the 1-hexanethiol concentration in the phase under consideration and in equilibrium with the 1-hexanethiol concen-

tration in the ionic liquid phase, respectively. The K_f represents the overall mass transfer coefficient (m s^{-1}), being the interfacial area of the cell, A_i (m^2), and the extraction time, t (s).

C_f^* is related with the 1-hexanethiol concentration in the ionic liquid rich phase (C_{IL}) through the distribution ratio (D), calculated using the experimental concentration of the feed and the ionic liquid phases at the equilibrium:

$$C_f^* = \frac{C_{IL}}{D} \tag{2}$$

A simple mass balance to the solute at the initial conditions is applied to obtain an expression for the concentration C_{IL}:

$$C_{IL} = \frac{V_f}{V_{IL}}(C_f^0 - C_f) \qquad t = 0, C_f = C_f^0, C_{IL} = C_{IL}^0 = 0 \tag{3}$$

where the C_f^0 and C_{IL}^0 are the concentration of 1-hexanethiol in the feed and ionic liquid phases, at the initi k_f al time, and is the ionic liquid phase volume.Substituting Eqs. (2) and (3) in (1), and integrating using the initial conditions, the overall mass transfer coefficient, K_f, can be determined by fitting the experimental concentrations of the thiol as a function of time.

The resistances-in-series model was used to estimate the overall mass transfer coefficient, based on the combination of the two individual mass transfer coefficients of both feed and ionic liquid boundary films, k_f and k_{IL}, respectively:

$$\frac{1}{K_f} = \frac{1}{k_f} + \frac{1}{Dk_{IL}} \tag{4}$$

Taking into account that the mass transfer in each phase depends on the hydrodynamic conditions, mass transfer correlations using the Sherwood (Sh), Reynolds (Re) and Schmidt (Sc) numbers were used to estimate the solute individual mass transfer coefficients.

The following correlation, described in Eq. (5), was selected to describe the individual mass coefficients, k, in the laminar layers occurring at each side of the interface of the two individual mechanically stirred phases [38–40].

$$Sh = 0.664\, Re^{1/2}Sc^{1/3} \tag{5}$$

The dimensional numbers of Sherwood, Reynolds and Schmidt are defined as $Sh = \frac{kd_i}{\mathfrak{D}}$, $Re = \frac{Nd_i^2\rho}{\mu}$ (impeller Reynolds number), $Sc = \frac{\mu}{\rho\mathfrak{D}}$, respectively.

$\mathfrak{D}$ is the diffusion coefficient of 1-hexanethiol in the feed (n-dodecane) or in the ionic liquid (m^2 s^{-1}), d_i and N are the impeller diameter (m) and speed (rad s^{-1}), and ρ and μ the density (kg m^{-3}) and the dynamic viscosity (Pa s) for each phase, respectively.

Information about the diffusion coefficient of liquids in ionic liquids is very scarce, and consequently, there are no specific correlations for the transport and molecular properties for this type of systems. Therefore, the Wilke–Chang correlation (Eq. (6)) was chosen to estimate the 1-hexanethiol diffusion coefficient in the ionic liquids tested, due to its vast and general application and good agreement with experimental values determined for organic solute diffusion in ionic liquids [41].

For the 1-hexanethiol diffusion coefficient in the n-dodecane solvent, the most suitable correlation for organic mixtures is the Scheibel correlation (Eq. (7)) [42].

$$\mathfrak{D}_{Wilke-Chang} = \frac{7.4 \times 10^{-8}(\varnothing M_{solv.})^{1/2}T}{\mu_{solv.}V_{RSH}^{0.6}} \tag{6}$$

$$\mathfrak{D}_{Scheibel} = 8.2 \times 10^{-8}\left(1 + \left(\frac{3V_{solv.}}{V_{RSH}}\right)^{0.66}\right)\frac{T}{\mu_{solv.}V_{RSH}^{0.33}} \tag{7}$$

In these expressions, $\mathfrak{D}_{Wilke-Chang}$ and $\mathfrak{D}_{Scheibel}$ are the mutual diffusion coefficient of solute 1-hexanethiol at very low concentrations in solvent ionic liquid or n-dodecane (cm^2 s^{-1}), by the

Wilke–Chang correlation or the Scheibel correlation, respectively, at a T temperature (K). The $M_{solv.}$ is the molecular weight of solvent ionic liquid or n-dodecane (g mol^{-1}), $\varnothing$ is the association factor of solvent, dimensionless, being 1 considering in this case the ionic liquid as non-associating compound, is the viscosity of solvent (mPa s), and V_{RSH}, $V_{solv.}$ are the molar volume (cm^3 mol^{-1}) of the solute 1-hexanethiol and the solvent ionic liquid or n-dodecane, respectively, at their normal boiling temperature (K).

Being the studied ionic liquids composed by organic ions, the Scheibel method was also applied to the thiol diffusion in the ionic liquids, for comparison of the estimated values.

The molar volume for the 1-hexanethiol, ionic liquid and n-dodecane, at their normal boiling temperature, are also values that needed to be estimated and were calculated by the Schroeder method [42].

3. Materials and methods

3.1. Materials

The model "jet-fuel" constituents selected were the hydrocarbon n-dodecane and the thiol 1-hexanethiol, 99% and 95% pure, respectively, from Sigma–Aldrich, Germany.

Three ionic liquids with different density and viscosity properties were tested: 1-ethyl-3-methylimidazolium methylsulfate, 1-ethyl-3-methylimidazolium triflate, and 1-ethyl-3-methylimidazolium bis (trifluoromethylsulfonyl)imide. All the ionic liquids were acquired at IoLiTec, Ionic Liquid Technology, Germany, with a purity superior to 99%. Before using, the ionic liquids were dried and purified by heating (313.15 K), under constant stirring and at moderate vacuum (1 mPa) for a minimum of 24 h.

Each ionic liquid content in water, after the drying procedure, and the respective physical properties are reported in Table 1.

3.2. Liquid–liquid extraction kinetic experiments

The extraction cell used for these studies consists of a modified Lewis cell [47,48] with a total volume of 22.8 ml. A double paddle vertical stirrer, 15 mm of diameter, promotes the individual phase mixing by a regulated motor with a tachometer (Model 461895, Extech Instruments). To maintain a constant temperature fixed at 298.2 K (±0.1 K), the cell is thermostatized by circulating water through a tube enfolding the cell. The water was thermo-regulated with a temperature stability of ±0.1 K by means of a thermostat bath circulator (Julabo MC).

The ionic liquid and the feed mixture (n-dodecane + 1-hexanethiol) were added to the extraction cell (11.4 ml each phase), remaining the ionic liquid as the lower phase, and the feed as the upper phase, due to their different densities (Table 1). Samples of each phase (0.3 ml) were collected simultaneously and analyzed at suitable intervals until the equilibrium was reached.

3.2.1. Analytical methods

The thiol concentration, in each phase, was analyzed by potentiometric titration (±2.6% for the n-dodecane rich phase and ±7.9% for the ionic liquid rich phase), using a TitraLab®865 titration workstation, with an alcoholic solution of AgNO$_3$ at 0.01 M, according to the ASTM D3227 standard [49]. This method has a detection threshold of 1 mol/m^3 for the thiol concentration for the sample volumes analyzed.

Supporting our previous work results [25], no peaks corresponding to the tested ionic liquid in the hydrocarbon-rich phase were found by UV spectroscopy. For the ionic-liquid-rich phase, also no dodecane was found by gravimetrical analysis (±10^{-4} g). Therefore, the content of ionic liquid and n-dodecane in the dodecane and

Table 1
Solvents (n-dodecane and ionic liquids) physical properties, at 298.2 K.

Solvent	$M_{solv.}$ (mol g^{-1})	w_{H_2O} (ppm)	$\rho_{solv.}$ (kg m^{-3})	$\mu_{solv.}$ (mPa s)
n-Dodecane	170.33	28.2	745.7[43]	1.36[43]
[C$_2$mim][MeSO$_4$]	222.3	130.1	1278.3[44]	84.19[44]
[C$_2$mim][CF$_3$SO$_3$]	260.2	305.2	1379.1[45]	40.58[45]
[C$_2$mim][NTf$_2$]	391.3	283.3	1519.3[46]	32.46[46]

Table 2
Membrane support specifications and properties.

Membrane support properties	Hydrophobic polyvinylidene fluoride (hb-PVDF)	Hydrophilic polyvinylidene fluoride (hl-PVDF)	Teflon (PTFE)	Polyethersulfone (PES)	Cellulose acetate (CA)	Polypropylene (PP)
	Millipore Corporation	Pall Corporation	Sartorius Stedim Biotech GmbH	Pall Corporation	GVS Group	Celgard®
Thickness (μm)	125	129	50.5	145	80	130
Pore diameter (μm)	0.22	0.20	0.2	0.2	0.22	0.05
Porosity (%)	70	80	30	80	70	30
Wettability to the ionic liquids	High	High	Low	High	Membrane is dissolved	Low

ionic liquid-rich phases, respectively, were considered negligible. Nevertheless, traces of these compounds might be present at each phase in concentrations below the detection threshold.

The water content of the solvents tested was determined by Karl–Fischer titration, using a Metrohm 831 Karl Fischer coulometer.

3.2.2. Calculation methods

The software package Matlab™, from Math Works Inc. (USA), was applied to perform the fitting of the thiol concentration variation with time, for the kinetic experiments, using the *nlinfit* routine. The overall mass transfer coefficients were determined performing a nonlinear regression, using the iterative least squares algorithm, and simultaneously solving the differential equations system specified in mass transfer modelling. The parameters' errors were calculated within a 95% confidence interval.

3.3. Supported ionic liquid membranes (SILMs) experiments

In order to assess the feasibility of the application of supported ionic liquid membranes for thiol desulfurization by a reduced pressure driven process, different ionic liquids and support membrane materials were investigated.

The ionic liquids studied comprised the previous ionic liquids of the liquid–liquid extraction experiments (1-ethyl-3-methylimidazolium methylsulfate, 1-ethyl-3-methylimidazolium triflate, and 1-ethyl-3-methylimidazolium bis (trifluoromethylsulfonyl)imide), in order to understand the impact of their properties on the stability and permeation behavior of the resulting supported liquid membranes [36].

In terms of membrane materials, the PVDF supports, with hydrophobic character or hydrophilic character by surface-modification, were already tested hitherto for gas separation processes [50,51] and a higher stability behavior was obtained for the hydrophobic PVDF. Hydrophilic PVDF and hydrophilic PES (treated surface membrane) with imidazolium ionic liquids were applied and compared in gas separation experiments [52] and long term stabilities were achieved for both materials. Nevertheless, in order to determine which support would be more appropriate to produce stable SILMs for this specific desulfurization task, stability experiments were carried out for these and other materials with different composition and properties, identified in Table 2, with the respective specifications and supplier.

3.3.1. SILMs preparation

The ionic liquid was immobilized on the support membranes by first removing the air from the pores of the membrane applying vacuum for 1 h on a stainless steel vacuum chamber, which facilitates the incorporation of the ionic liquids into the porous structure. After spreading ionic liquid drops on the membrane surface, still under vacuum and, after stabilization for at least 1 h, the SILM excess of ionic liquid was removed using a tissue. The amount of ionic liquid incorporated was determined gravimetrically, and the membrane thickness change due to swelling was also measured using a micrometer Metric z169048, Sigma–Aldrich, Spain (±5 μm).

3.3.2. SILMs characterization

Regarding the supported ionic liquid membranes characterization, the weight and thickness of the membrane, before and after the immobilization procedure, were measured using an analytical balance Sartorius A.G. Göttingen CP225D, Germany (±10^{-4} g), and a micrometer Metric z169048, Sigma–Aldrich, Spain (±5 μm), respectively.

The contact angle of 1-ethyl-3-methylimidazolium triflate in the hydrophobic polyvinylidene fluoride and polypropylene supports were also measured using a sessile drop method measured by a KSV's CAM 101 goniometer, which captures and automatically analyses video images for the contact angles measured.

3.3.3. SILMs stability

The SILMs stability was investigated by two different techniques, which allowed to evaluate the ionic liquid displacement from the membrane support by the permeation of air, as a result of a pressure gradient applied to the membrane system.

The first set of experiments consisted in measuring the SILM ionic liquid loss when submitted to a pressure higher than atmospheric pressure. For this, the SILMs were placed in a dead-end filtration cell (10 mL AmiconTH ultrafiltration unit), and a nitrogen stream was used to apply pressure up to 2 bar in the feed circuit. At regular periods of time, the SILMs were weighed, using a Sartorius balance (A.G. Göttingen CP225D, Germany), to determine the reduction of the SILM weight caused by ionic liquid losses.

The second type of experiments was carried out in a stainless steel flat circular unit composed by two compartments, separated by the SILM. A lower pressure was applied to the downstream compartment, while the upper compartment was exposed to air. After stabilization of the pressure in the downstream compart-

ment, vacuum was cut and the pressure evolvement, due to the permeation through the membrane, was registered over time. The SILMs were weighed before and after this experimental procedure, also to measure the ionic liquid loss.

3.3.4. Permeation through the SILMs

The permeation behavior of the components of the jet-fuel model through the SILMs is an important aspect to be considered, since these SILMs must present a high selectivity to be viable for a membrane assisted desulfurization process.

The n-dodecane permeation tests were performed in a stainless steel flat circular module. This unit is composed by two compartments that were separated by the SILM. To evaluate the SILM stability using organic solvents, after applying vacuum at the downstream compartment and stabilization of the pressure, the upper compartment was filled with n-dodecane. Then, the vacuum was cut and the pressure evolvement over time was registered. The SILM was also weighed before and after this experimental procedure.

4. Results and discussion

In consequence of the extremely low mutual solubility between the alkanes and the ionic liquids, and despite the low thiol partition for these extracting solvents, shown in our previous work [25], that makes the conventional liquid–liquid extraction process unviable, the liquid extraction process was here evaluated using a supported ionic liquid membrane.

Due to the importance of the extraction kinetics on this process, this section presents the study of the diffusion and mass transfer of 1-hexanethiol to the selected imidazolium based ionic liquids. In order to evaluate the application of SILMs in the membrane extraction process, their stability and selectivity are also analyzed testing the aforementioned ionic liquids and different support materials.

4.1. Liquid–liquid extraction kinetics

To further understand the thiol mass transfer between the hydrocarbon phase and the selected ionic liquids, extraction experiments were carried out with different ionic liquids, in a modified Lewis cell, previously described.

The experimental 1-hexanethiol concentrations (C_{RSH}, mol m^{-3}) in the dodecane and ionic liquid phases during the extraction process, for the ionic liquids [C$_2$mim][MeSO$_4$], [C$_2$mim][CF$_3$SO$_3$], and [C$_2$mim][NTf$_2$], are depicted in Fig. 1. The different experiments were carried out at a fixed stirrer speed of 200 rpm, to not disturb the interface, and at a constant temperature of 298.2 K. The thiol concentration was measured for the dodecane and ionic liquid rich phase, except for the samples with concentration of thiol below the detection threshold.

4.1.1. Mass transfer kinetics

By fitting the experimental concentrations of the feed phase with the set of differential equations (Eqs. 1–3), the overall mass transfer coefficient was determined for each system studied. The respective distribution ratio values were calculated by using the experimental concentration at the equilibrium for the feed and the ionic liquid phases (Fig. 1). The values obtained for each parameter are gathered in Table 3.

Regarding the mass transfer kinetics, the values obtained for the fitted overall mass transfer coefficients were $0.67 \pm 0.32 \times 10^{-7}$ m s^{-1}, $1.72 \pm 0.80 \times 10^{-7}$ m s^{-1}, and $2.01 \pm 0.48 \times 10^{-7}$ m s^{-1}, for the systems with the ionic liquids [C$_2$mim][MeSO$_4$], [C$_2$mim][CF$_3$SO$_3$], and [C$_2$mim][NTf$_2$], respectively (Table 3). From these fitted coefficients, and analyzing the 1-hexanethiol concentration profile plots (Fig. 1), the extraction rates observed can be considered as low, taking between 5 and 20 h to achieve the concentration plateau for the various systems tested.
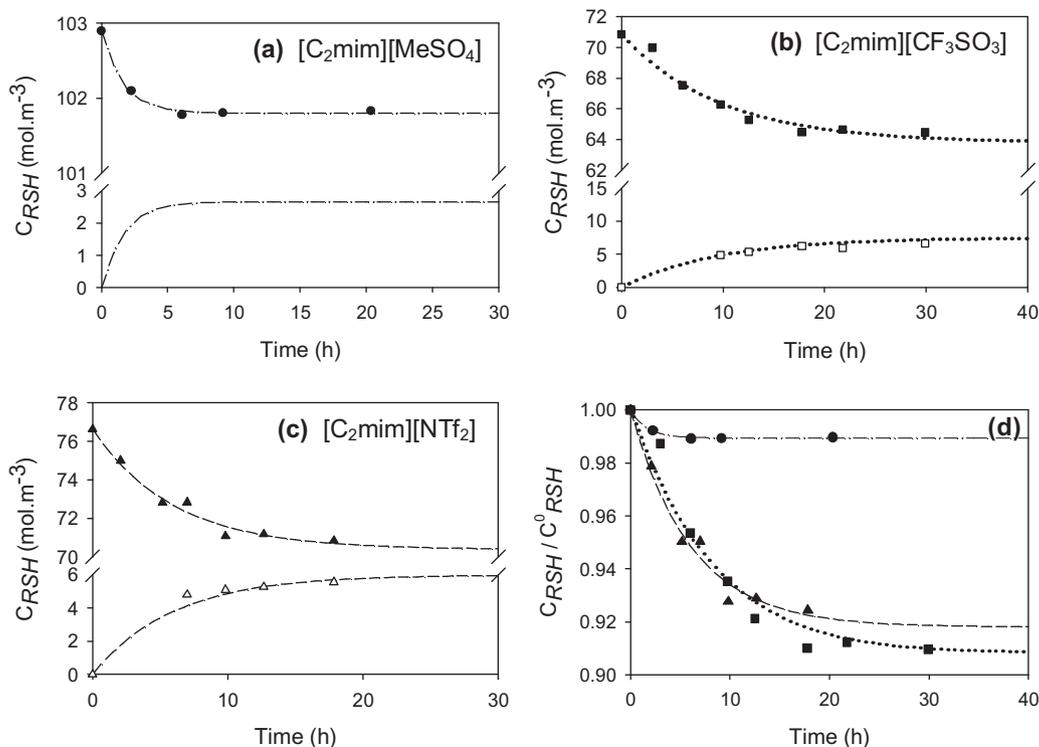

Fig. 1. 1-Hexanethiol experimental concentration profile in the dodecane and ionic liquid rich-phases (filled and empty symbols, respectively), and data fitting (lines) at 298.2 K and atmospheric pressure, using different extracting ionic liquids: (a) [C$_2$mim][MeSO$_4$] (circles and dot-dashed line), (b) [C$_2$mim][CF$_3$SO$_3$] (squares and dotted line), (c) [C$_2$mim][NTf$_2$] (triangles and dashed line). And (d) comparison between the three extraction systems studied (dodecane phase).

Table 3
Overall mass transfer and coefficient distribution ratio for the systems ionic liquid + 1-hexanethiol + n-dodecane, at 298.2 K and atmospheric pressure.

Ionic liquid	$\mu_{solv.}$ (mPa s)	$K_{f,exp.} \times 10^7$ (m s^{-1})	D
[C$_2$mim][MeSO$_4$]	84.19 [44]	0.67 ± 0.32	0.010 ± 0.008
[C$_2$mim][CF$_3$SO$_3$]	40.58 [45]	1.72 ± 0.80	0.095 ± 0.026
[C$_2$mim][NTf$_2$]	32.46 [46]	2.01 ± 0.48	0.079 ± 0.017

Table 4
Estimated diffusion of 1-hexanethiol in the n-dodecane and several ionic liquids, by the Scheibel ($\mathfrak{D}_{Scheibel}$) and the Wilke–Chang ($\mathfrak{D}_{Wilke–Chang}$) correlations, with the molar volume at the boiling point temperature calculated by the Schroeder correlation.

Solvent	$\mu_{solv.}$ (mPa s)	$\mathfrak{D}_{Scheibel}$ (m^2 s^{-1})	$\mathfrak{D}_{Wilke–Chang}$ (m^2 s^{-1})
n-Dodecane	1.36 [43]	1.20×10^{-9}	–
[C$_2$mim][MeSO$_4$]	84.19 [44]	1.86×10^{-11}	1.86×10^{-11}
[C$_2$mim][CF$_3$SO$_3$]	40.58 [45]	3.83×10^{-11}	4.12×10^{-11}
[C$_2$mim][NTf$_2$]	32.46 [46]	5.60×10^{-11}	6.38×10^{-11}

Given that the operating conditions are similar for the individual experiments, the differences observed are directly related with the ionic liquid tested, and consequently, with their physical properties. The behavior observed is determined by the ionic liquids viscosity, which has a significant impact on the mass transfer coefficients. In fact, high ionic liquid viscosities are responsible for increasing the boundary layer immediately adjacent to the interface, hindering the molecular transport in this region [39]. Consequently, the decrease of the ionic liquid viscosity contributes for the mass transfer coefficients increase from [C$_2$mim][MeSO$_4$], [C$_2$mim][CF$_3$SO$_3$], to [C$_2$mim][NTf$_2$].

Additionally and as supported by the resistances-in-series model, the distribution coefficient within also attains a large contribution in the overall mass transfer coefficients. For the systems studies, this impact is be estimated to be between 10 and 100.

Regarding the distribution ratio, the values obtained were low due to the low solubility of the 1-hexanethiol in the tested ionic liquids (Table 3). The [C$_2$mim][MeSO$_4$] ionic liquid shows the lowest distribution ratio, with a value of 0.010 ± 0.008, whereas the [C$_2$mim][CF$_3$SO$_3$] and the [C$_2$mim][NTf$_2$] exhibit higher values, 0.095 ± 0.026 and 0.079 ± 0.017, respectively. Comparing these results with the distribution ratios obtained by ternary liquid–liquid equilibrium experiments in our recent work [25], the values found are in accordance (0.010 ± 0.007, 0.113 ± 0.009 and 0.115 ± 0.011, values converted from molar fraction ratio to concentration ratio, as defined in Eq. (2)).

The low distribution ratios observed are a result of the weak interactions between the 1-hexanethiol and the ionic liquids in study. The n-dodecane and the 1-hexanethiol are essentially non- and very low polar molecules, respectively, where the main intermolecular interactions are van der Waals forces, albeit the thiol can also involve less significant dipole–dipole interactions, due to the individual –SH group. On the other hand, much different electrostatic and hydrogen-bonding type interactions occur in the ionic liquids. Combining these compounds, the interactions between them contemplate essentially week dispersive forces and dipole–dipole attractions. Since the cation [C$_2$mim]$^+$ is common in the ionic liquids tested, the differences observed are related with anions mostly due to their different polarity. Here anions with lower polarity tend to interact through dispersive van der Waal forces, which promote a better affinity between the thiol and the ionic liquid. A more extensive explanation on the thiol/alkane/ionic liquid interaction can be found in our prior work [25]. Nonetheless, it is necessary to have in mind that fuels are a very complex mixture, and improving the affinity of ionic liquids to the target compounds for extraction, can also lead to increasing the undesirable ability to extract alike fuel compounds.

4.1.2. Mass transfer correlations

The individual mass transfer coefficients were estimated using the Sherwood correlation for the laminar layers at the system interface (Eq. (5)). To apply this correlation, the 1-hexanethiol diffusion coefficients in the feed and ionic liquid phases were evaluated using the Scheibel and the Wilke–Chang correlation, respectively. The calculated values are shown in Table 4. The results estimated are in the order of 10^{-9} m s^{-1} in the feed phase and two orders lower (10^{-11} m s^{-1}) in the different ionic liquids

studied. This is a consequence of the significative differences on the solvents viscosity, being superior two orders of magnitude for the ionic liquids. For the systems tested, the n-dodecane viscosity is slightly higher than 1 mPa s, whereas for the ionic liquids, it is superior to 30 mPa s.

In the case of the feed n-dodecane, the diffusion coefficient is consistent with others reported in the literature for diffusion of solvents in organic solvents [42]. For the ionic liquids, the data on liquid diffusion coefficients in ionic liquids are still very scarce and, in spite of the diffusivity coefficient deviations encountered, the values here estimated are in the same range of other values reported in the literature for solute diffusivity in ionic liquids [31,53]. It is also noticeable that, the diffusion of the thiol in the ionic liquids depends from the ionic liquids viscosity. Regarding the comparison between the use of the Wilke–Chang or the Scheibel correlations, the estimated diffusion coefficients are very similar.

Having estimated the diffusion coefficients, the individual mass transfer coefficients were predicted by the Sherwood correlation described in Eq. (5). The mass transfer coefficients were obtained by summing the individual mass transfer coefficients (Eq. (4)). All values determined are shown in Tables 5a and b, with the respective Reynolds, Schmidt and Sherwood numbers.

For the systems studied, the values determined for the individual mass transfer coefficients in the laminar layer in the feed phase side, are identical and have a magnitude in the order of 10^{-5} m s^{-1}. With concern to the ionic liquid phase film, the values obtained are one order lower than the feed phase, standing on 10^{-6} m s^{-1}.

Since the inverse of these estimated individual mass transfer coefficients, weighted by the respective distribution coefficients (Eq. (4)), reflects the resistance of the 1-hexanethiol transport through the phase films, it is possible to state that the solute founds higher resistances for mass transfer in the ionic liquid phase. Also, in light of the selected Sherwood correlation, combined with the equation of the resistances-in-series model, it is also possible to infer about the controlling step. Therefore, independent variation of the phases' hydrodynamics shows that the rate of 1-hexanethiol extraction is controlled by the ionic liquid phase.

Analyzing specifically the ionic liquid phase, the low mass transfer coefficients are determined by the viscosity, as can be seen by the viscosity contribution to the decrease of the diffusion coefficients (Table 4), and the reduced agitation degree (low Reynolds numbers), which are responsible for a slow thiol transport in a thick boundary layer. For the tested ionic liquids, the individual mass transfer coefficients increase following the order [C$_2$mim][MeSO$_4$], [C$_2$mim][CF$_3$SO$_3$], and [C$_2$mim][NTf$_2$], obeying to the decrease of the viscosity and the respective increase of the diffusivity.

With relation to the overall mass transfer coefficients, a good agreement between the experimental and the estimated values by the selected Sherwood correlation was achieved.

From the previous experiments, it was possible to conclude that, due to the very slow extraction rates of the thiol compound from the feed to the ionic liquid along with the low partition of

Table 5a
Estimated individual mass transfer coefficients for the several tested ionic liquids, with the respective Reynolds, Schmidt and Sherwood numbers determined.

Ionic liquid	Feed phase				Ionic liquid phase						
	Re	Sc_{Sche}	Sh_{Sche}	$k_f \times 10^5$ (m s^{-1})	Re	$Sc_{Sche} \times 10^5$	$Sc_{Wc} \times 10^5$	Sh_{Sche}	Sc_{WC}	$k_{IL_{She}} \times 10^6$ (m s^{-1})	$k_{IL_{WC}} \times 10^6$ (m s^{-1})
[C$_2$mim][MeSO$_4$]	2871	1518	406	3.25	80	35.11	35.05	898	898	1.11	1.11
[C$_2$mim][CF$_3$SO$_3$]	2806	1518	401	3.21	172	7.77	7.22	795	777	2.03	1.98
[C$_2$mim][NTf$_2$]	2754	1518	398	3.19	235	3.82	3.35	734	703	2.74	2.62

Note: the subscripts Sche and WC indicate if the value estimated was calculated using the Scheibel or the Wilke–Chang diffusion coefficient, respectively.

Table 5b
Estimated and experimental overall mass transfer coefficients for the several tested ionic liquids.

Ionic liquid	Overall mass transfer		
	Estimated		Experimental
	$k_{f_{Sche}} \times 10^7$ (m s^{-1})	$k_{f_{WC}} \times 10^7$ (m s^{-1})	$K_{f,exp} \times 10^7$ (m s^{-1})
[C$_2$mim][MeSO$_4$]	0.11	0.11	0.67 ± 0.32
[C$_2$mim][CF$_3$SO$_3$]	1.92	1.87	1.72 ± 0.80
[C$_2$mim][NTf$_2$]	2.15	2.06	2.01 ± 0.48

Note: the subscripts Sche and WC indicate if the value estimated was calculated using the Scheibel or the Wilke–Chang diffusion coefficient, respectively.

the 1-hexanethiol towards the ionic liquid, the use of conventional liquid–liquid extraction equipment is discouraged in real conditions as a viable separation process, since it would require high operation time and very high volume of ionic liquid to achieve the mandatory thiol limits in the fuel.

On the other hand, the negligible mutual solubility between the majority aliphatic compounds of jet-fuel compounds, as is the *n*-dodecane, and the large variety of ionic liquids, still makes very attractive the application of these non-volatile solvents for the removal of thiols. Thus, the addition of a regeneration step of the ionic liquid to the liquid–liquid extraction process might overcome the problems perceived, since the ionic liquid might be continuously cleaned, promoting a higher concentration gradient and a separation process kinetically controlled.

In view of these considerations, the next section presents the extraction of thiols using supported ionic liquid membranes as an alternative approach to the desulfurization process.

4.2. Supported ionic liquid membrane experiments

The extraction of 1-hexanethiol from the fuel stream by the selected ionic liquids can be performed using supported ionic liquid membranes (SILMs). The ionic liquid confined inside the pores of the membrane works as a liquid membrane and, by applying vacuum on the permeated side, the 1-hexanethiol selectively solubilizes and diffuses across the ionic liquid and is continuously stripped.

With regard to the SILMs requisites, such as chemical and mechanical resistance, and high selectivity to the target solute, SILMs are expected to benefit from the almost negligible mutual solubility between the aliphatic hydrocarbons and ionic liquids. In this way, the ionic liquid will work as a carrier to the target compounds and, due to the differences between the thiol and the dodecane partition, their separation should occur in a very selective mode, with a minimal volume of ionic liquid, filling the porous supporting membrane [35,54].

Nevertheless, as stated before, the instability of supported liquid membranes is usually a critical issue for industrial application. For the separation in question, the SILMs should exhibit long term integrity with no liquid losses nor swelling and degradation of the supporting membrane material, and favorable transport towards the target solute.

4.2.1. Membrane support
Both hydrophobic and hydrophilic polyvinylidene fluoride (PVDF) and the polyethersulfone (PES) supports are easily wettable by the tested ionic liquids. Fig. 2a) shows the low contact angle of the [C$_2$mim][CF$_3$SO$_3$] ionic liquid on the hydrophobic membrane of PVDF. For the ionic liquid incorporation in polypropylene (PP) and Teflon (PTFE) membrane supports, the method and/or period of immobilization used in this work were not effective. This can be explained by the smaller pores of the PP support and higher hydrophobicity of the PTFE support, that promote lower wettability (high contact angle) of the supports by the ionic liquids (Fig. 2b for the PP support)). As for the cellulose acetate (CA) support, it was visually observed a physical degradation of the support material.

The incorporation of ionic liquid into the hydrophobic PVDF, hydrophilic PVDF and PES supports resulted in an increase of the weight and thickness of the membranes, as can be seen in Table 6. The weight variation corresponds to the necessary amount of ionic liquid to fill the pores, and the thickness expansion is related to the swelling effect of the ionic liquid in the support material, being more pronounced when the hydrophilic PVDF support was used.

4.2.2. Ionic liquid losses
In order to evaluate the integrity of the SILMs when operated under pressure differences due to ionic liquid displacement from the membrane support pores, two different approaches were used.
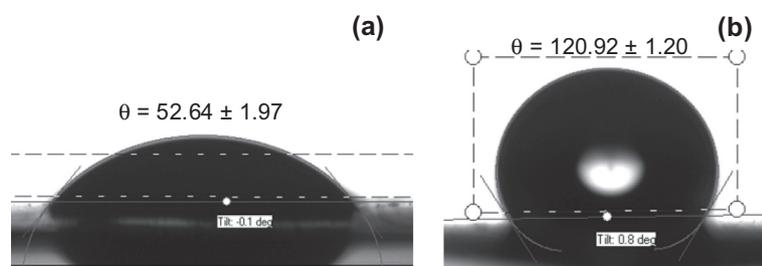

(a) θ = 52.64 ± 1.97

(b) θ = 120.92 ± 1.20

Fig. 2. Contact angle of the ionic liquid [C$_2$mim][CF$_3$SO$_3$] with (a) the hydrophobic PVDF membrane, and (b) the PP membrane.

Table 6
Weight increase (Δm%) and thickness ($\Delta \delta$%) after immobilization.

		[C$_2$mim][MeSO$_4$]	[C$_2$mim][CF$_3$SO$_3$]	[C$_2$mim][NTf$_2$]
		(2745.3 ppm H$_2$O, μ = 84.17 mPa s)	(1020.8 ppm H$_2$O, μ = 39.38 mPa s)	(202.9 ppm H$_2$O, μ = 32.46 mPa s)
Hydrophobic PVDF SILM	Δm%	141.9	154.7	179.1
	$\Delta \delta$%	5.4	9.0	17.3
Hydrophilic PVDF SILM	Δm%	252.3	273.7	310.7
	$\Delta \delta$%	11.3	13.5	22.4
PES SILM	Δm%	–	386.8	–
	$\Delta \delta$%	–	9.6	–

In the first set of experiments, a positive pressure difference is applied using a nitrogen gas stream in the feed compartment; in the second case, the SILM was submitted to a negative pressure difference (vacuum in the downstream compartment). In both cases, the SILM weight was measured before and after the experiment.

From the positive pressure difference experiments, Fig. 3 shows that the SILMs prepared with hydrophobic PVDF support are more stable than the ones prepared with hydrophilic PVDF. As can be seen, the ionic liquid loss from the hydrophobic support is lower than 4% for all the ionic liquids tested up to 2 bar, with exception of the [C$_2$mim][MeSO$_4$]/hb-PVDF SILM, that start showing a more pronounced ionic liquid displacement after 1.5 bar of pressure difference. When comparing the ionic liquids tested, it can be concluded that the [C$_2$mim][CF$_3$SO$_3$]/hb-PVDF SILM is the most stable membrane, presenting losses lower than 2% up to 1.4 bar, followed by the [C$_2$mim][NTf$_2$] up to 1 bar. These losses are extremely low and they may be due to a removal of excess of ionic liquid from the membrane surface and not to a displacement of ionic liquid from the membrane pores.

When filling the feed compartment of the permeation cell with air at atmospheric pressure and applying vacuum in the downstream side (negative pressure difference), an increase of the permeate pressure side is observed due to air permeation through the SILM (Fig. 4), as a result of air solubility in the ionic liquid. A linear pressure profile confirms that the membrane pores are totally filled with the ionic liquid since no abrupt gas leak is observed. Moreover, it indicates that no pronounced removal of the ionic liquid from pores of the membrane occurs. The losses observed are lower than 0.7%, 2.2% and 4.7%, for the [C$_2$mim][MeSO$_4$], [C$_2$mim][CF$_3$SO$_3$, and [C$_2$mim][NTf$_2$]-SILMs, respectively.

Fig. 4. Pressure profile in the permeate side, when applying a negative pressure difference across the hydrophobic PVDF/ionic liquid SILM. Feed compartment: air at atmospheric pressure; Downstream compartment: vacuum at a starting pressure of 0.9 mbar.

4.2.3. Permeation through SILMs

The thiol removal from fuel requires the highest SILM selectivity possible, i.e., a high permeability for the target thiols and very low, rather negligible, permeation of the hydrocarbons. Based on the jet-fuel model assumed in this work, the pure n-dodecane permeation across the studied SILMs was evaluated in first place.

Taking into account the results of the good and stable ionic liquid incorporation in the membrane support, the hydrophobic PVDF membrane support was tested with the ionic liquid [C$_2$mim][CF$_3$SO$_3$], due to its low mutual solubility with aliphatic hydrocarbons, aiming to assure no permeation these compounds. The experimental results obtained for the hydrophobic PVDF/[C$_2$mim][CF$_3$SO$_3$] are plotted in Fig. 5 a), represented by the full square symbols. They show the pressure increase in the permeate side during operation time, which results from the n-dodecane permeation across the SILM. This result was unexpected given the high stability of the SILM prepared with this specific membrane support and ionic liquid. The observed permeation of n-dodecane cannot be explained by a displacement of ionic liquid from the membrane pores.

In order to understand the undesirable transport of n-dodecane through the hydrophobic PVDF-based SILMs, other support materials were evaluated, namely hydrophilic PVDF (aiming at increasing the polarity of the SILM), and PES. Still, the results were unsatisfactory in both cases, as depicted in Fig. 5a). For these SILMs, a faster n-dodecane permeation through the [C$_2$mim][CF$_3$SO$_3$] hydrophilic SILM was even observed, and the ionic liquid loss with the hydrophilic PVDF and PES supports was higher (7.4% wt. and 8.7% wt., respectively).

As the permeation of n-dodecane could not be attributed to transport through empty pores, due to ionic liquids displacement, neither transport through the ionic liquid itself (as result of the extremely low affinity of n-dodecane to the ionic liquids), it was decided to investigate the transport of n-dodecane through the
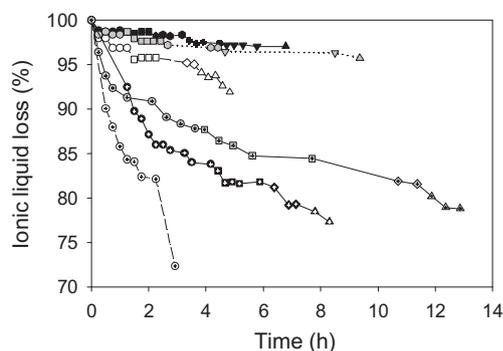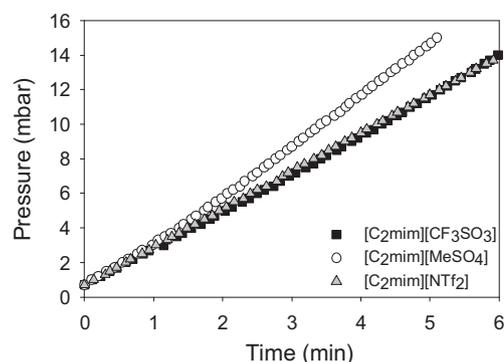

Fig. 3. SILM ionic liquid loss along time, for the SILMs composed by PVDF hydrophobic (full symbols) and hydrophilic (dotted symbols), with the ionic liquids [C$_2$mim][CF$_3$SO$_3$] (black symbols and solid line), [C$_2$mim][NTf$_2$] (grey symbols and dot-dashed line), and [C$_2$mim][MeSO$_4$] (white symbols and dashed line), for positive pressure differences of 0.5 bar (circles), 1.0 bar (squares), 1.4 bar (hexagons), 1.5 bar (diamonds), 1.6 bar (cross), 1.8 bar (inverse triangles), and 2.0 bar (triangles), using a nitrogen gas stream on the AmiconTH 8010 cell.
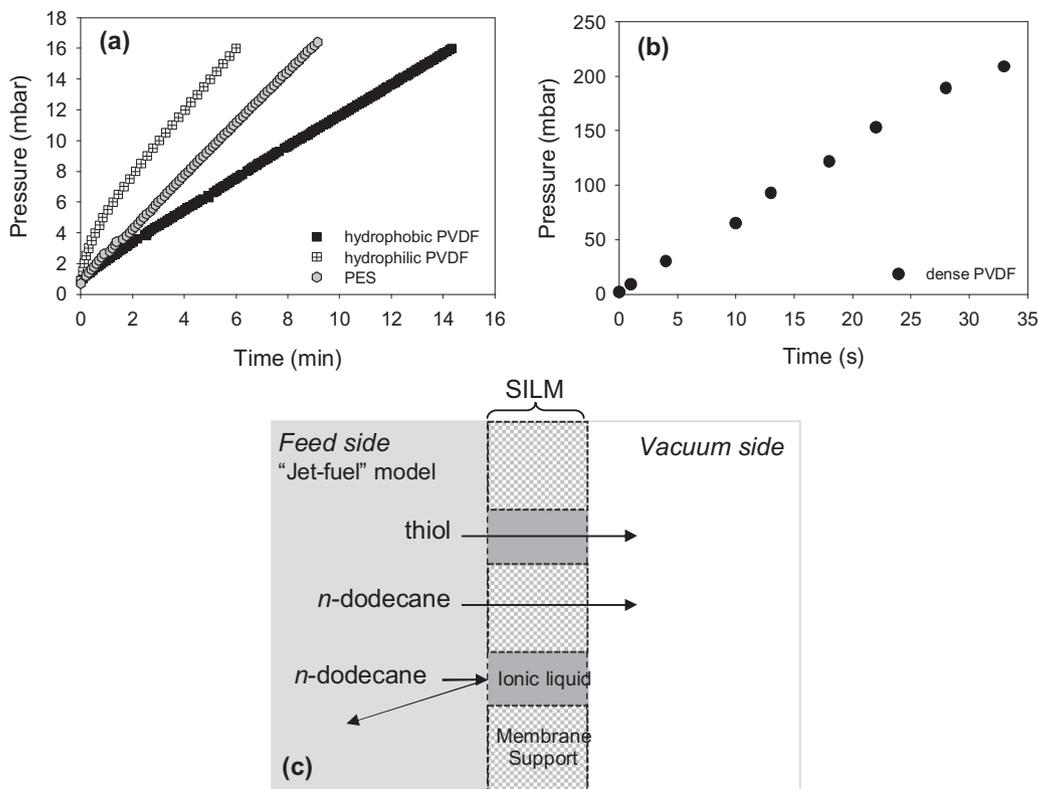
Fig. 5. Pressure profile in the permeate side, for the *n*-dodecane permeation when applying a negative pressure difference across (a) [C₂mim][CF₃SO₃]-based SILMs with different membrane supports; and (b) a dense PVDF membrane. A proposed scheme for the *n*-dodecane transport occurring in SILMs is illustrated in (c).

polymeric materials that constitute the supporting porous membrane.

To understand if the *n*-dodecane SILM permeation was due to the support, a dense PVDF membrane was used in the reduced pressure unit. It was found that the PVDF polymer is extremely permeable to *n*-dodecane, as can be seen by the very fast pressure increase in the permeate side (Fig. 5b)). Comparing Fig. 5(a) and (b), it can be concluded that the ionic liquid in the pores of the membrane acts as a barrier to the *n*-dodecane transport, as can be inferred from the different operation time to achieve the same pressure increase of 16 mbar. While for the tested SILMs it requires between 5 and 16 min, for the dense PVDF, it is almost instantaneous. Therefore, it may be concluded that although the membrane

pores are well impregnated with ionic liquid, *n*-dodecane permeation occurs through the membrane support material.

Fig. 5c) explains how the transport of *n*-dodecane take place in SILMs.

To overcome the undesirable permeation of the alkane through the polymer, an alternative could be the use of ionic liquid as an additional barrier after the SILM, in order to block the *n*-dodecane crossing over to the permeate side. This approach is shown in a schematic illustration in Fig. 6. In this approach a membrane wettable or non-wettable by the ionic liquid can be used, however, the overall resistance to the thiols transport must be evaluated. Considering the study carried out in this work concerning the mass transfer of the 1-hexanethiol from the feed phase to the ionic
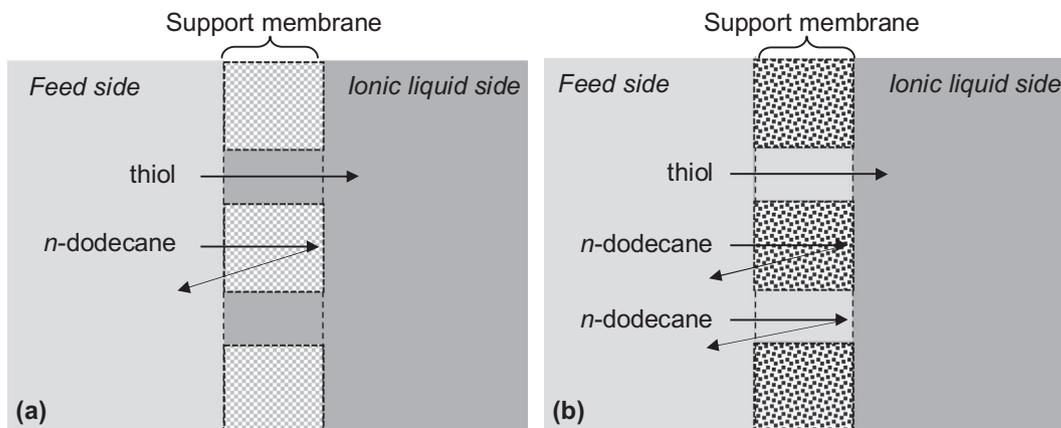

Fig. 6. Thiol and *n*-dodecane transport through the membrane under different operating modes with an ionic liquid as the receptor phase, using (a) a membrane wetted or (b) a membrane not wetted by the ionic liquid.

liquid, from which it was concluded that the dominant resistance to the thiol transport occurs in the ionic liquid, it would be more adequate the use of a non-wettable membrane by the ionic liquid, in order to reduce the resistance in the membrane, as shown in Fig. 6b). In both cases, the alkanes presented in the "jet-fuel" are expected to not permeate to the receiving ionic liquid phase.

Taking into account the previous discussion, a membrane not wetted by the selected ionic liquid ([C_2mim][CF_3SO_3]) was evaluated. The experiments were carried out in a Liqui-cel MiniModule® Contactor with microporous polypropylene hollow fiber membranes (Celgard® X-10), circulating the feed phase in the shell side and the ionic liquid inside of the fibres.

With this configuration, no *n*-dodecane was detected in the ionic liquid phase, eliminating the problem of *n*-dodecane transport. Additionally, the use of this equipment favors the extraction step of the process since it promotes a very high surface area/volume ratio of transport (3225 m^2/m^3), reducing the extraction time from 20 to 2 h. Fig. 7 shows the transport of the target solute 1-hexanethiol from the *n*-dodecane feed phase to the ionic liquid phase, when operating this equipment.

Having in mind the mass transfer steps taking place in the extraction process with SILMs, the mass transfer mechanism can be decoupled into simultaneous actions in two membrane contactors. This methodology consists in the use of a first membrane contactor in which occurs the selective extraction of the target solute from the feed phase, without losses of other fuel constituents (as shown). Then, the ionic liquid with the extracted thiol can be regenerated in a second membrane contactor, by applying vacuum or using a sweep gas in the downstream compartment. This step should allow for a complete cleaning of the ionic liquid allowing its reuse in the extraction step. Integrating both steps, the ionic liquid circulates in a closed loop between both membrane contactors, requiring therefore much lower volumes of ionic liquid than in conventional equipment. Additionally, this configuration allows for maximizing of the concentration driving force, making possible a continuous desulfurization of the fuel feed.

5. Conclusions

This work addressed the study of ionic liquids for the removal of thiols from jet-fuel streams. As the affinity of the thiols compounds towards the ionic liquids is relatively low, high volumes of extracting ionic liquid would be required in conventional liquid–liquid extraction. This requirement turns the conventional process unviable.
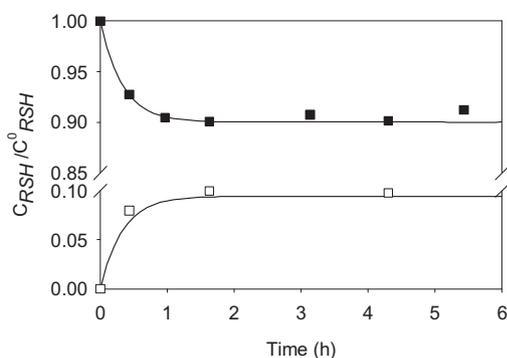

Fig. 7. 1-Hexanethiol experimental concentration profile in the *n*-dodecane feed phase (filled squares) and ionic liquid receiving phase (empty squares), for the extraction in a Liqui-cel MiniModule® Contactor with microporous polypropylene hollow fiber membranes (Celgard® X-10), at 298.2 K and atmospheric pressure. Shell side: jet-fuel model (1-hexanethiol + *n*-dodecane); Lumen side: ionic liquid ([C_2mim][CF_3SO_3]).

This work proposes an alternative method. It was investigated the incorporation of ionic liquid in the pores of a membrane support (supported ionic liquid membrane – SILM) to be applied in the extraction of thiols from a jet-fuel model stream, composed by a mixture of 1-hexanethiol and *n*-dodecane. Making use of the ionic liquids' negligible volatility and their very low mutual solubility with the aliphatic compounds, SILMs can be applied in a separation process in which vacuum is applied in the downstream side to remove the thiol selectively extracted by the SILM.

To understand the transport behavior of the thiol from the *n*-dodecane-rich phase to the ionic liquid, extraction experiments were carried out testing an ionic liquid from the family of the 1-ethyl-3-methylimidazolium cation. The systems tested presented low mass transfer coefficients, 0.67×10^{-7} m s^{-1}, $1.72 \pm 0.80 \times 10^{-7}$ m s^{-1} and $2.01 \pm 0.48 \times 10^{-7}$ m s^{-1} for the systems with [C_2mim][$MeSO_4$], [C_2mim][CF_3SO_3] and [C_2mim][NTf_2], respectively, controlled by the thiol transport in the ionic liquid phase. This behavior can be overcome due to the permanent removal of the ionic liquid in the SILM to the receiving phase.

The stability behavior of SILMs was also evaluated. The tested SILMs demonstrated an efficient immobilization of the ionic liquid and a good stability when using an organic feed and applying vacuum. However, the permeation of *n*-dodecane observed through the SILM polymeric support was noteworthy, even though the negligible mutual solubility between the *n*-dodecane and the studied ionic liquids.

This problem was surpassed by using ionic liquid as a receiving phase in the downstream side of a hollow fibre membrane contactor, in counter-flow with the feed stream. The ionic liquid tested was [C_2mim][CF_3SO_3], which has a very low mutual solubility with *n*-dodecane and, as a result, no dodecane was detected in the ionic liquid phase. This work opens the possibility for an integrated extraction/stripping of thiols from "jet-fuel" streams by using two membrane contactors in series, where extraction to a selected ionic liquid takes place in the first contactor, and stripping from the ionic liquid occurs in a second contactor. Using this configuration, the ionic liquids used can be continuously regenerated and recycled between both contactors.

References

[1] B. Pawelec, R.M. Navarro, J.M. Campos-Martin, J.L.G. Fierro, Towards near zero-sulfur liquid fuels: a perspective review, Catal. Sci. Technol. 1 (2011) 23–42.
[2] EIA U.S., Crude oils have different quality characteristics, 2012 <http://www.eia.gov/todayinenergy/detail.cfm?id=7110>. (Last access: 15 April 2014.).
[3] J. Griffin, A.-M. Fantini, K. Aylward-Marchant, World Oil Outlook 2013, OPEC, Austria, 2013.
[4] M. Francisco, A. Arce, A. Soto, Ionic liquids on desulfurization of fuel oils, Fluid Phase Equilib. 294 (2010) 39–48.
[5] P.S. Kulkarni, C.A.M. Afonso, Deep desulfurization of diesel fuel using ionic liquids: current status and future challenges, Green Chem. 12 (2010) 1139–1149.
[6] C. Song, An overview of new approaches to deep desulfurization for ultra-clean gasoline, diesel fuel and jet fuel, Catal. Today 86 (2003) 211–263.
[7] V.C. Srivastava, An evaluation of desulfurization technologies for sulfur removal from liquid fuels, Rsc. Adv. 2 (2012) 759–783.
[8] M. Zhang, W. Zhu, S. Xun, H. Li, Q. Gu, Z. Zhao, Q. Wang, Deep oxidative desulfurization of dibenzothiophene with POM-based hybrid materials in ionic liquids, Chem. Eng. J. 220 (2013) 328–336.

[9] M. Zhang, W. Zhu, H. Li, S. Xun, W. Ding, J. Liu, Z. Zhao, Q. Wang, One-pot synthesis, characterization and desulfurization of functional mesoporous W-MCM-41 from POM-based ionic liquids, Chem. Eng. J. 243 (2014) 386–393.

[10] K.S. Triantafyllidis, E.A. Deliyanni, Desulfurization of diesel fuels: adsorption of 4,6-DMDBT on different origin and surface chemistry nanoporous activated carbons, Chem. Eng. J. 236 (2014) 406–414.

[11] F. Subhan, B.S. Liu, Acidic sites and deep desulfurization performance of nickel supported mesoporous AlMCM-41 sorbents, Chem. Eng. J. 178 (2011) 69–77.

[12] P. Li, L. Zhao, P. Wei, S. Li, H. Qu, J. Lee, Y. Kong, H. Sun, Mass transfer of hydroxyethyl cellulose membranes for desulfurization of FCC gasoline: experimental and modeling, Chem. Eng. J. 231 (2013) 255–261.

[13] Z.E.A. Abdalla, B. Li, Preparation of MCM-41 supported (Bu4N)4H3(PW11O39) catalyst and its performance in oxidative desulfurization, Chem. Eng. J. 200–202 (2012) 113–121.

[14] W.D. Liang, S. Zhang, H.F. Li, G.D. Zhang, Oxidative desulfurization of simulated gasoline catalyzed by acetic acid-based ionic liquids at room temperature, Fuel Process. Technol. 109 (2013) 27–31.

[15] Z.W. Jin, S. Wang, J.Q. Wang, M.X. Zhao, Effects of plasticization conditions on the structures and properties of cellulose packaging films from ionic liquid [BMIM]Cl, J. Appl. Polym. Sci. 125 (2012) 704–709.

[16] J.L. Wang, D.S. Zhao, K.X. Li, Extractive desulfurization of gasoline using ionic liquid based on CuCl, Petrol. Sci. Technol. 30 (2012) 2417–2423.

[17] F.T. Li, Y. Liu, Z.M. Sun, L.J. Chen, D.S. Zhao, R.H. Liu, C.G. Kou, Deep extractive desulfurization of gasoline with xEt(3)NHCl center dot FeCl3 ionic liquids, Energy Fuel 24 (2010) 4285–4289.

[18] L. Alonso, A. Arce, M. Francisco, O. Rodriguez, A. Soto, Gasoline desulfurization using extraction with [C-8 mim][BF4] ionic liquid, AIChE J. 53 (2007) 3108–3115.

[19] C.P. Huang, B.H. Chen, J. Zhang, Z.C. Liu, Y.X. Li, Desulfurization of gasoline by extraction with new ionic liquids, Energy Fuel 18 (2004) 1862–1864.

[20] E. Kuhlmann, M. Haumann, A. Jess, A. Seeberger, P. Wasserscheid, Ionic liquids in refinery desulfurization: comparison between biphasic and supported ionic liquid phase suspension processes, Chemsuschem 2 (2009) 969–977.

[21] M.F. Taha, N. Atikah, F.K. Chong, M.S. Shaharun, Oxidative desulfurization of dibenzothiophene from model oil using ionic liquids as extracting agent, AIP Conf. Proc. 1482 (2012) 258–262.

[22] L.H. de Oliveira, V.H. Alvarez, M. Aznar, Liquid–liquid equilibrium in N-Methyl-2-hydroxyethylammonium acetate, butanoate, or hexanoate ionic liquids plus dibenzothiophene plus n-dodecane systems at 298.2 K and Atmospheric Pressure, J Chem. Eng. Data 57 (2012) 744–750.

[23] N.R. Varma, A. Ramalingam, T. Banerjee, Experiments, correlations and COSMO-RS predictions for the extraction of benzothiophene from n-hexane using imidazolium-based ionic liquids, Chem. Eng. J. 166 (2011) 30–39.

[24] S. Werner, M. Haumann, P. Wasserscheid, Ionic liquids in chemical engineering, Annu. Rev. Chem. Biomol. 1 (2010) 203–230.

[25] A.R. Ferreira, M.G. Freire, J.C. Ribeiro, F.M. Lopes, J.G. Crespo, J.A.P. Coutinho, Ionic liquids for thiols desulfurization: experimental liquid–liquid equilibrium and COSMO-RS description, Fuel 21 (2014) 21–24.

[26] L.A. Neves, N. Nemestóthy, V.D. Alves, P. Cserjési, K. Bélafi-Bakó, I.M. Coelhoso, Separation of biohydrogen by supported ionic liquid membranes, Desalination 240 (2009) 311–315.

[27] P. Scovazzo, J. Kieft, D.A. Finan, C. Koval, D. DuBois, R. Noble, Gas separations using non-hexafluorophosphate [PF6](−) anion supported ionic liquid membranes, J. Membr. Sci. 238 (2004) 57–63.

[28] A. Seeberger, C. Kern, A. Jess, Gas desulfurization by supported ionic liquid membranes (SILMs), Oil Gas-Eur. Mag. 35 (2009) 94–100.

[29] A.P. de los Rios, F.J. Hernandez-Fernandez, L.J. Lozano, S. Sanchez-Segado, A. Ginesta-Anzola, C. Godinez, F. Tomas-Alonso, J. Quesada-Medina, On the selective separation of metal ions from hydrochloride aqueous solution by pertraction through supported ionic liquid membranes, J. Membr. Sci. 444 (2013) 469–481.

[30] K.F. Kilulya, T.A.M. Msagati, B.B. Mamba, J.C. Ngila, T. Bush, Ionic liquid–liquid extraction and supported liquid membrane analysis of lipophilic wood extractives from dissolving-grade pulp, Chromatographia 75 (2012) 513–520.

[31] G.O. Yahaya, F. Hamad, A. Bahamdan, V.V.R. Tammana, E.Z. Hamad, Supported ionic liquid membrane and liquid–liquid extraction using membrane for

[32] R. Fortunato, M.J. Gonzalez-Munoz, M. Kubasiewicz, S. Luque, J.R. Alvarez, C.A.M. Afonso, I.M. Coelhoso, J.G. Crespo, Liquid membranes using ionic liquids: the influence of water on solute transport, J. Membr. Sci. 249 (2005) 153–162.

[33] L.J. Lozano, C. Godínez, A.P. de los Ríos, F.J. Hernández-Fernández, S. Sánchez-Segado, F.J. Alguacil, Recent advances in supported ionic liquid membrane technology, J. Membr. Sci. 376 (2011) 1–14.

[34] P. Luis, L.A. Neves, C.A.M. Afonso, I.M. Coelhoso, J.G. Crespo, A. Garea, A. Irabien, Facilitated transport of CO2 and SO2 through supported ionic liquid membranes (SILMs), Desalination 245 (2009) 485–493.

[35] M.A. Malik, M.A. Hashim, F. Nabi, Ionic liquids in supported liquid membrane technology, Chem. Eng. J. 171 (2011) 242–254.

[36] R. Fortunato, C.A.M. Afonso, M.A.M. Reis, J.G. Crespo, Supported liquid membranes using ionic liquids: study of stability and transport mechanisms, J. Membr. Sci. 242 (2004) 197–209.

[37] P.S. Kulkarni, L.A. Neves, I.M. Coelhoso, C.A.M. Afonso, J.G. Crespo, Supported ionic liquid membranes for removal of dioxins from high-temperature vapor streams, Environ. Sci. Technol. 46 (2012) 462–468.

[38] G.J. Lye, D.C. Stuckey, Extraction of erythromycin-A using colloidal liquid aphrons: Part II. Mass transfer kinetics, Chem. Eng. Sci. 56 (2001) 97–108.

[39] J.R. Welty, C.E. Wicks, R.E. Wilson, G.L. Rorrer, Fundamentals of Momentum, Heat, and Mass Transfer, John Wiley & Sons Inc, Hoboken, 2008.

[40] R.E. Treybal, Mass-Transfer Operations, McGraw-Hill, Michigan, 1955.

[41] J. Bedia, E. Ruiz, J. de Riva, V.R. Ferro, J. Palomar, J. Jose Rodriguez, Optimized ionic liquids for toluene absorption, Aiche J. 59 (2013) 1648–1656.

[42] R.C. Reid, J.M. Prausnitz, B.E. Poling, The properties of gases and liquids, 4th ed., McGraw-Hill, New York, 1987.

[43] E.W. Lemmon M.O.M.a.D.G.F., Thermophysical properties of fluid systems, in: P.J. Linstrom, W.G. Mallard (Ed.), NIST Chemistry WebBook, NIST Standard Reference Database Number 69, National Institute of Standards and Technology, Gaithersburg.

[44] A. Bhattacharjee, C. Varanda, M.G. Freire, S. Matted, L.M.N.B.F. Santos, I.M. Marrucho, J.A.P. Coutinho, Density and viscosity data for binary mixtures of 1-Alkyl-3-methylimidazolium alkylsulfates + water, J. Chem. Eng. Data 57 (2012) 3473–3482.

[45] H. Rodríguez, J.F. Brennecke, Temperature and composition dependence of the density and viscosity of binary mixtures of water + ionic liquid, J. Chem. Eng. Data 51 (2006) 2145–2155.

[46] C. Schreiner, S. Zugmann, R. Hartl, H.J. Gores, Fractional walden rule for ionic liquids: examples from recent measurements and a critique of the so-called ideal KCl line for the Walden Plot†, J. Chem. Eng. Data 55 (2009) 1784–1788.

[47] J.B. Lewis, The mechanism of mass transfer of solutes across liquid-liquid interfaces: Part I: the determination of individual transfer coefficients for binary systems, Chem. Eng. Sci. 3 (1954) 248–259.

[48] R. Taylor, R. Krishna, Multicomponent Mass Transfer, John Wiley & Sons Inc, New York, 1993.

[49] ASTM D3227 – Standard Test Method for (Thiol Mercaptan) Sulfur in Gasoline, Kerosine, Aviation Turbine, and Distillate Fuels (Potentiometric Method), in, ASTM International, 2013.

[50] L.A. Neves, J.G. Crespo, I.M. Coelhoso, Gas permeation studies in supported ionic liquid membranes, J. Membr. Sci. 357 (2010) 160–170.

[51] J. Albo, E. Santos, L.A. Neves, S.P. Simeonov, C.A.M. Afonso, J.G. Crespo, A. Irabien, Separation performance of CO2 through Supported Magnetic Ionic Liquid Membranes (SMILMs), Sep. Purif. Technol. 97 (2012) 26–33.

[52] P. Scovazzo, D. Havard, M. McShea, S. Mixon, D. Morgan, Long-term, continuous mixed-gas dry fed CO2/CH4 and CO2/N2 separation performance and selectivities for room temperature ionic liquid membranes, J. Membr. Sci. 327 (2009) 41–48.

[53] H.R. Cascon, S.K. Choudhari, 1-Butanol pervaporation performance and intrinsic stability of phosphonium and ammonium ionic liquid-based supported liquid membranes, J. Membr. Sci. 429 (2013) 214–224.

[54] R.D. Noble, D.L. Gin, Perspective on ionic liquids and ionic liquid membranes, J. Membr. Sci. 369 (2011) 1–4.